Audio Engineering Society

# Conference Paper

Presented at the Conference on
Automotive Audio
2017 September 8 – 10, San Francisco, CA, USA



# On acoustical modeling and validation of automotive loudspeaker grilles

Martin Olsen[1], Peter John Chapman[1], Michal K. Bogdanski[2], and Michael Strauss[2]

[1]*Harman Lifestyle Audio, Struer, Denmark*
[2]*Harman Virtual Product Development, Straubing, Germany*

Correspondence should be addressed to Martin Olsen (martin.olsen@harman.com)

### ABSTRACT

This paper addresses prediction techniques for evaluating the consequences of adding a grille assembly onto a loudspeaker. Numerical modeling is applied in order to assess the acoustical effects imposed on the loudspeaker sub-system defined as a loudspeaker, interface, and grille. Investigations are performed in a virtual infinite baffle scenario under semi-anechoic conditions, where various modeling aspects are included in the studies. The predictions are shown to accurately reproduce the prominent features of the sub-system when compared with experimental data. The paper highlights the intricacies of both measurement and correct modeling of the geometry of the parts and their acoustic properties – particularly at higher audio frequencies.

## 1 Introduction

The prevalence of advanced numerical simulation tools has enabled acoustical engineers to adapt rapid development iteration cycles and establishes a creative link between engineering and industrial design. One benefit of introducing such procedures is the increased potential in achieving cutting edge industrial design solutions while maintaining, or even improving, the acoustics of the resulting sound system. In many products, available on the market today, loudspeaker grilles constitute the primary artistic canvas of the audio system, since these create the visual interface between the loudspeakers and the interior design of the car cabin (along with the user interface). Accordingly, the loudspeaker grilles are currently one of the most important design elements, seen from the branded audio perspective, providing brand identity and differentiation.

The loudspeaker grille assembly normally consists of a loudspeaker mounting piece, the grille part, and an interface coupling the loudspeaker to the grille. Traditionally, the main focus has been on evaluating the resulting acoustic transparency of the grille part, by estimating the difference in the on-axis response (or several points defining a listening window) with and without the grille in front of the loudspeaker compared to the mechanical degree of openness in the structure. However, when utilized for evaluating the resulting performance in the automotive domain, this approach might turn out to be non-exhaustive. The reason behind this is the packaging of loudspeakers in the car interior, where a scattered loudspeaker layout is often employed along the geometrically complex boundaries of the cabin. This introduces the requirement of a more detailed assessment of the grille assembly, where the resulting coupling to the in-situ acoustical environment plays an important role, and is heavily depending on the spatial frequency of the problem.

The listening scenario inside the car cabin differs significantly from the loudspeaker/listener configuration in domestic rooms. In the automotive domain, the orientation of the loudspeaker often results in an off-axis listening situation. It is of particularly high importance to take into account the sound energy, which is not directly distributed towards the ears of the listener. This is mainly due to the complex acoustical environment, where the distances to adjacent oddly shaped boundaries are short, and that the boundaries possess very different acoustical properties [1].

In the present paper, the loudspeaker grille assessment is addressed mainly for high frequency loudspeakers. The nature of the radiated wave field makes careful evaluation of the resulting system more relevant compared, for example, with low frequency loudspeaker assemblies. However, different effects occur in the low frequency scenario such as rattling and turbulence. In the case of midrange loudspeakers a combination of the effects described above often applies.

Previously, modeling the effects of adding a grille assembly to a loudspeaker has been done by adding a resistive load as radiation condition in a lumped parameter dynamic loudspeaker model, generally treated in [2]. Numerical modeling of the problem, based on 3-D geometries in a virtual environment, is relevant since the specific geometrical features can be included by means of defining the discretization of the problem. In the present work, a finite element model is considered based a on pressure acoustics domain formulation.

The paper is structured as follows: In Sec. 2 an overview of the theory of the sound radiation problem is presented in relation to finite element analysis modeling. The method applied to the loudspeaker grille assessment, considered in this paper, is described in Sec. 3, including both simulation and measurement studies. The results are provided in Sec. 4, and discussed in the context of the automotive audio application in Sec. 5. Conclusive remarks are given in Sec. 6.

## 2 Theory

In the present section, the underlying fundamental theory of the sound radiation problem, considered in the following studies, is summarized. Simulation methods employing wave-based formulations are utilized. The wave equation is solved with the appropriate boundary conditions in a discretized spatial domain, resembling the physical parts to be evaluated, the Finite Element Method (FEM). A sketch of the domains is shown in Fig. 1. For FEM-based simulations, meshed volumes are providing the discretization, and defines the resulting air domains where wave propagation occurs, as indicated by the gray regions in Fig. 1. The resulting mathematical formulation is given by a large, sparse matrix problem to be solved. An alternative formulation of the problem is the Boundary Element Method (BEM), where only a boundary mesh is required, but results in a small but dense mathematical problem. The FEM simulation approach was found advantageous over the BEM for the specific application, due to small spatial regions and the access to efficient iterative solvers. A detailed presentation of the underlying theory of numerical simulation methods in general is omitted here, but the reader is referred to [3] and [4]. Instead, a brief overview of the governing equations in relation to interior/exterior domain formulations will be provided here, along with a brief introduction of the relevant boundary conditions.

The governing equation for the physics of the interior domain, here denoted $\Omega_{int}$ (and indicated by dark gray shading in Fig. 1), is the frequency domain version of the inhomogeneous wave equation, or equivalently the Helmholtz equation [5], given by

$$\nabla^2 p(\mathbf{x}) + k^2 p(\mathbf{x}) = Q_m, \quad \mathbf{x} \in \Omega_{int}, \tag{1}$$

where $k$ is the wave number related to the radian fre-

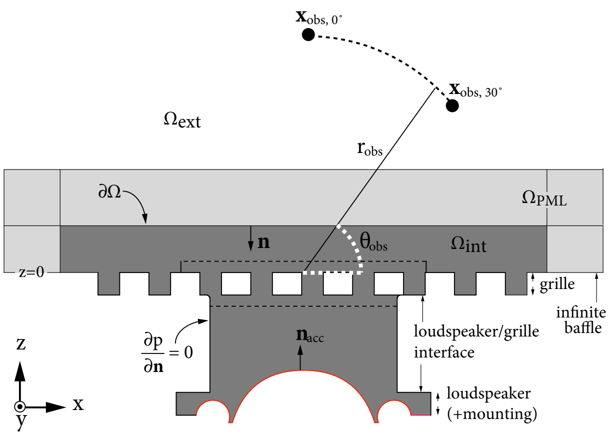


**Fig. 1:** Illustration of the section view through the finite element domains defined for the radiation problem of concern. The observation points are computed in the exterior domain, outside the gray FEM-regions.

quency $\omega$ and the speed of sound $c$, and $Q_m$ is a monopole source term. For the numerical problem, the wavelength, $\lambda = 2\pi/k$, of the wave-solutions must be resolved by appropriate discretization of the spatial domains in which the solution is computed.

Since frequency domain pressure acoustics simulations are adopted in the present studies, the primary boundary conditions are defined as:

- **the sound hard boundary**, hence the gradient of sound pressure normal to the boundary equals zero:

$$\mathbf{n} \cdot \nabla p(\mathbf{x}) = 0 \tag{2}$$

- **the acoustic impedance**, $Z_{imp}$, defined as the ratio of acoustic pressure and normal velocity on the specific boundary:

$$-\mathbf{n} \cdot \left( -\frac{\nabla p(\mathbf{x})}{\rho} \right) = \frac{i\omega p(\mathbf{x})}{Z_{imp}}, \tag{3}$$

- **the interior perforated plate**, which in the special case of a loudspeaker grille part consisting of cylindrical holes in a uniformly distributed layout, can be approximated with a simplified model of the grille provided by an impedance model. An interior perforated thin plate of thickness $t_p$ can be characterized by a transfer impedance, which is given by the ratio of pressure drop across to the particle velocity on the boundary $u_n$, denoted as:

$$\begin{aligned} Z_{imp,p} = &-\mathrm{Re}(f_1(\omega, t_p, \sigma)) \\ &- i\,\mathrm{Im}(f_2(\omega, t_p, \sigma)) + f_3(\sigma, u_n), \end{aligned} \tag{4}$$

  where $\sigma$ is the ratio of perforated area to grille plate area, and the dummy functions $f_{1-3}$ are introduced here for the sake of simplicity. The functions represent transfer impedance of a cylindrical hole, flow and area porosity, and non-linear and mean flow effects, treated in details in [6].

- **the normal acceleration** of a given surface, describing a simplified acoustic source, where no feed-back or mechanical features are included.

The infinite baffle scenario is realized by means of a sound pressure symmetry condition in the xy-plane, where the loudspeaker grille assembly is flush mounted. The exterior domain is defined outside a small air domain located above the infinite baffle and the outer surface of the grille. Perfectly matched layers (PML) are attached to the air domain (denoted $\Omega_{PML}$ in Fig. 1), and introduces an open and non-reflecting infinite domain for sound radiation via coordinate transformation [7]. This is a general radiation condition not limited to specific types of outgoing wave fields. The governing equation of the problem in the source-free exterior domain $\Omega_{ext}$, bounded by the closed surface $\partial\Omega$, is the homogeneous Helmholtz equation, or equivalently Eq. 1 with $Q_m = 0$. The solution $p(\mathbf{x})$ to homogeneous Helmholtz equation can be explicitly expressed by means of the Kirchoff-Helmholtz integral equation [5], given as

$$p(\mathbf{x}) = \int_{\partial\Omega} \left( G(\mathbf{x}_s, \mathbf{x}) \nabla p(\mathbf{x}_s) - \nabla G(\mathbf{x}_s, \mathbf{x}) p(\mathbf{x}_s) \right) \cdot \mathbf{n}\, d\partial\Omega, \tag{5}$$

where $G(\mathbf{x}_s, \mathbf{x})$ denotes the free-field Greens function with source position $\mathbf{x}_s$. The integral equation states that knowing the complex sound pressure and pressure gradient at the enclosing boundary $\partial\Omega$, the solution $p(\mathbf{x})$ can be determined for all $\mathbf{x} \notin \Omega_{int}$ without loss of generality. Hence, all relevant observation points for the simulation studies, presented in the following sections, rely on post-processing utilizing the numerical solution on $\partial\Omega$ evaluated in the observation points of interest by evaluating Eq. 5.

## 3 Methods

A validation study was conducted in order to investigate the accuracy of simulation models, with the purpose of predicting the effect of adding loudspeaker grille assemblies in automotive loudspeaker systems. The present study considers a high frequency 19 mm loudspeaker, including one type of grille with interface and a reference scenario. The geometries are shown in Fig. 2. The specific part consists of a cylindrical grille interface of height 12 mm, and a 3 mm grille part with holes of 3 mm diameter. The hole pattern is interlaced (or triangular) with a hole to plate ratio of 67%. The loudspeaker grille assembly selected here reflects a common geometry often applied in automotive implementations. A reference case is comprised by the loudspeaker mounting part from the grille assembly without grille and interface, as shown in Fig. 2a.

All samples, both in simulation and measurement studies, were evaluated in a $2\pi$-baffle setup, at a radial distance of $r_{obs} = 0.3$ m and at angles $\theta_{obs} \in \{-60°, -55°, \ldots, 60°\}$ in the horizontal plane, and defines the evaluation points for the directivity plots as indicated in Fig. 1. The frequency region of interest is

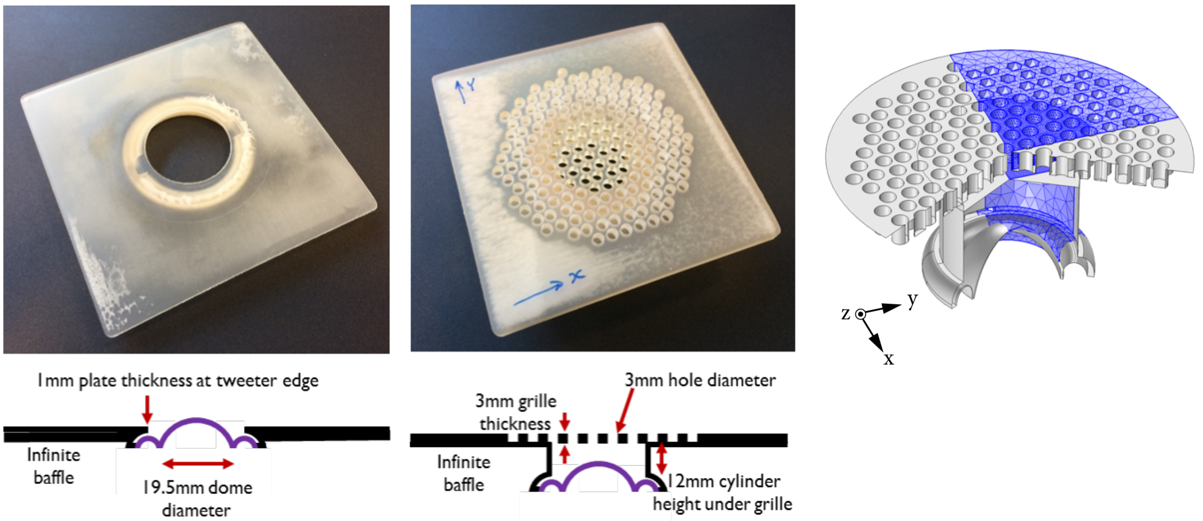


**(a)** Reference scenario.

**(b)** Loudspeaker grille test part.

**(c)** Illustration of the mesh used in the simulation of the grille assembly, when symmetry conditions are applied.

**Fig. 2:** An overview of the two loudspeaker grille types and the reference scenario utilized in the simulation studies and 3D-printed parts for validation measurements.

$f \in [2, 20]$ kHz.

The simulations were performed using a commercial FEM software package (Comsol Multiphysics). Numerical modeling of the loudspeaker grille assembly was obtained by means of a pressure acoustics frequency domain model in three spatial dimensions. The radiation problem was evaluated in the exterior domain in the observation points of concern, according to Fig. 1. The interior domain is defined as the air domain outlining the boundary of the loudspeaker membrane, the inner boundaries of the grille interface, including the holes defining the grille perforation. An example of the mesh of the interior domain is found in Fig. 2c. It should be noticed that wave propagation from the loudspeaker and interface is only occurring directly through the center part of the grille (where also high mesh density is seen), as the remainder of the holes are blind as illustrated in Fig. 2b. The higher mesh density, compared to the remainder of the interior domain, resolves the narrow spatial features around the grille part.

The following assumptions have been applied to the model:

- The loudspeaker is modeled as a simple two-dimensional normal acceleration, on the geometrical boundary of the loudspeaker membrane.

- All parts of the assembly are sound hard, hence all mechanical vibration phenomena have been neglected, which is reasonable for high frequency loudspeakers at low excitation levels.

- Symmetry considerations were applied, in all three (x,y,z) planes, were utilized in order to reduce the computational effort, as indicated by the quarter-domain mesh shown in Fig. 2c.

- The infinite baffle condition is obtained by means of symmetric sound pressure on each side of the xy-plane.

Experimental studies were conducted in order to validate the predictions based on the numerical simulations. Two parts were 3-D-printed based on the 3-D geometries (CAD-data) imported in the numerical simulation setup, and fitted with a high frequency loudspeaker, a Tymphany 0x20SC00-04 19 mm dome tweeter. The specific loudspeaker was common for all measurement series, hence individual loudspeaker variations are not present among the setups. The measurement system consisted of a 1/2-inch microphone, Brüel & Kjær type 4133, located on a measurement rig in front of a $2\pi$-baffle in a large $(12x12x12)m^3$ measurement room with dampened walls, described in [8]. The measurement procedure was based on the logarithmic sine sweep method described in [9], utilizing a MATLAB implementation with RME Fireface 800 sound card as interface. The impulse response measurement routine had a sweep time of one second (400 Hz - 22 kHz) with two repetitions and two pre-averages. Due to the short distance of 0.3 m between the loudspeaker grille under test and the microphone, a time-window was applied to each of estimated impulse responses in order to capture only the prominent features of the loudspeaker system.

## 4 Results

In this section, the predictions from the simulation studies and the experimental results are shown and compared. All responses presented here have been smoothed in 1/12-octave bands, and the absolute level of the simulation results has been aligned with the sound pressure level in the measurements. In Fig. 3a the measured and simulated on-axis frequency response are shown for the reference case. The simulated response agrees well with the measurement above 5 kHz, and the main features are predicted e.g. the dip found just above 14 kHz and the increasing trend towards 20 kHz. The directivity prediction and measurement are seen in Fig. 3b and Fig. 3c, respectively. It is apparent that the the prediction shows the spatial baffle step, which indicates the transition from the directivity of the systems being determined primarily by the geometry of the mounting plate, to being controlled by the inherent directivity of the loudspeaker. The overestimation of the level above 14 kHz in the prediction is potentially due to a relative increase of the inherent directivity imposed by the simple normal acceleration description of the sound source. The on-axis frequency response of the loudspeaker grille assembly is found in Fig. 4a. The most prominent features are all predicted by the simulation, at similar frequencies compared to the measurement, however with certain variations in the level especially above 15 kHz. The directivies are shown in Fig. 4b and Fig. 4c, where it is seen that the overall trends in the sound radiation characteristics of the grille assembly are predicted.

In order to isolate the effects imposed by the grille assembly, a common comparison often seen is the decibel difference plot. The difference of the grille assembly and the reference case is seen in Fig. 5a. High correlation is found when comparing the predicted effect to the one determined experimentally on 3-D printed parts. Some minor discrepancies, of less than 2 dB, are seen at the peaks and dips above 10 kHz. A more

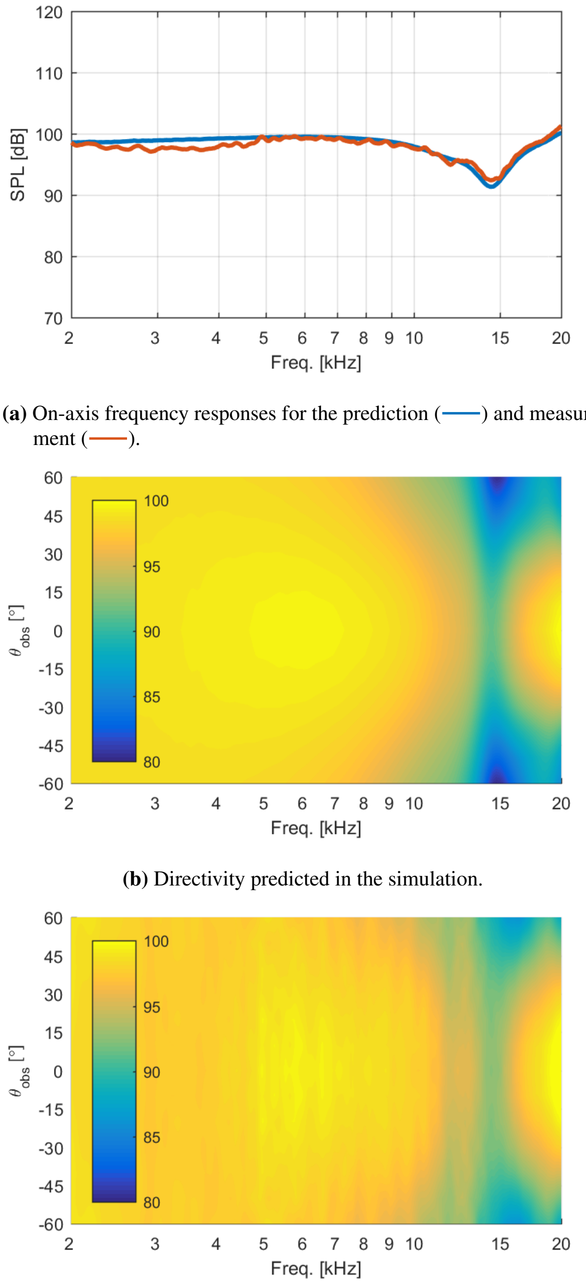


**(a)** On-axis frequency responses for the prediction (——) and measurement (——).



**(b)** Directivity predicted in the simulation.

**(c)** Measured directivity.

**Fig. 3:** Results obtained for the reference case including simulation and experimental data. The color scale shows dB SPL.

comprehensive comparison is shown in Fig. 5b and Fig. 5c, which can be interpreted as the 'finger print' of

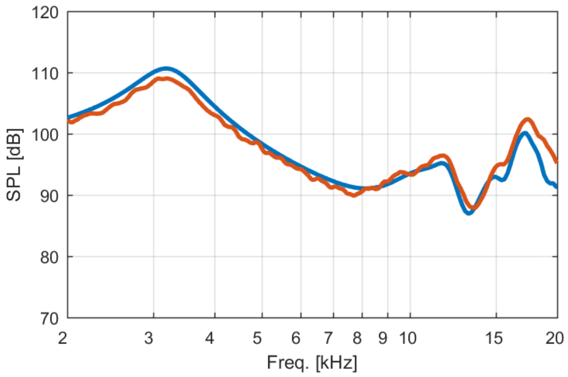


**(a)** On-axis frequency responses for the prediction (——) and measurement (——).

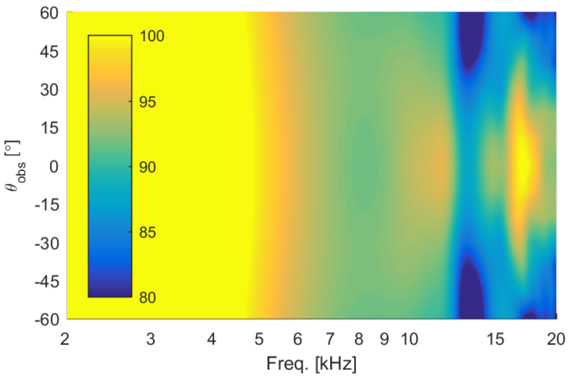


**(b)** Directivity predicted in the simulation.

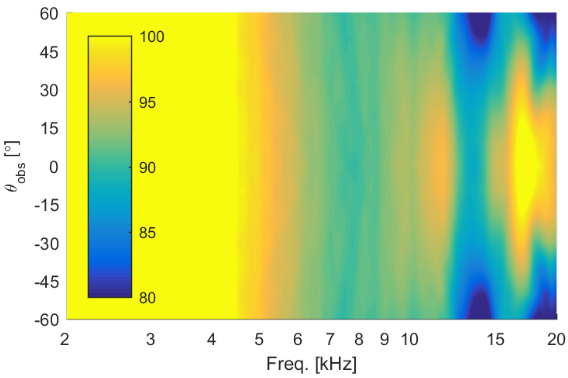


**(c)** Measured directivity.

**Fig. 4:** Results obtained for the grille assembly including simulation and experimental data. The color scale shows dB SPL.

the particular grille assembly under test. It is found that the main trends regarding the change in characteristics of sound radiation when adding the loudspeaker grille interface and grille part to the system are predicted well.

## 5 Discussion

The results presented in the previous section indicate that numerical modeling can be utilized in rapid assessment of loudspeaker grille assemblies. The prominent features of the system are all identified in the correct frequency regions, with similar magnitude compared to measurements, apart from minor deviations. In addition to the on-axis frequency response evaluation, the sound radiation characteristics are considered in more details by means of the directivity, which is an important aspect of the sound system elements in automotive sound systems. The importance of evaluating the dispersion of sound energy in relation to the acoustic environment and the specific packaging of the loudspeaker in the car interior, is high when optimizing the end-user experience. Furthermore, the simulation models enable the engineer to investigate the prominent details, which are normally not accessible in measurements conducted exterior to the part under consideration. Moreover, uncertainties in the measurements of the physical parts will mask attempts of detailed investigations of small but important features; something which is possible in the simulation domain. In practical measurement scenarios, it is expected that the measurement uncertainty in estimating a frequency response is approximately $\pm 0.5$ dB SPL [10]. Above 10 kHz the uncertainty is expected to be in the order of $\pm 1$ dB. Consequently, it can be expected that experimental errors in the setup, including the loudspeaker, grille assembly, and baffle, exhibit errors of the magnitude above.

The computational effort scales significantly depending on the number of details included in the simulation. A comparison of the on-axis frequency response predictions, based on different simulation approaches, is shown in Fig. 6. The main features of the response are highlighted and denoted A-D. The full 3-D representation of the grille geometry includes a mesh resolving the entire domain including each individual hole in the pressure acoustics domain, requiring the highest computational effort among the approaches considered here. Since the specific grille consists of uniformly distributed cylindrical holes, the simplified 2-D boundary condition, the interior perforated plate, can be applied which reduces the geometry complexity significantly. Consequently, if the interface is rotational symmetric, the numerical formulation is 2-D axis symmetric. The

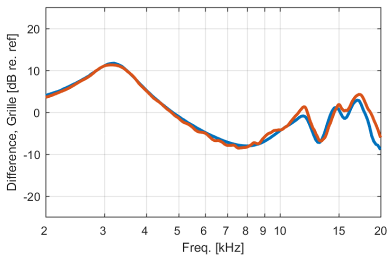


**(a)** Comparison of the difference on-axis frequency responses (with grille - w/o grille) for the simulation (——) and the measured reponsese (——).

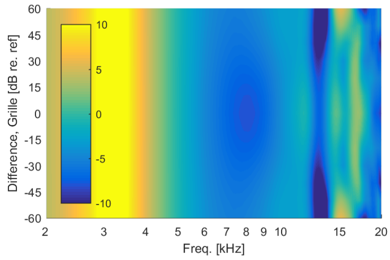


**(b)** Difference directivity (dB difference: grille minus no grille) for the simulated response.

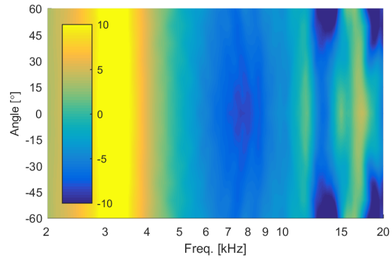


**(c)** Difference directivity (dB difference: grille minus no grille) for the measured response.

**Fig. 5:** Difference plots indicating the effect of adding a grille assembly to the reference case obtained by means of simulation and experimental data.

overall shape of the response is predicted using the boundary condition, however, the level above the feature A is overestimated and feature D is shifted upwards in frequency. The individual effects imposed by the interface and grille respectively, can be investigated by comparing the dashed black line (no grille) with the blue line. It is evident that feature A and C are introduced by the interface, whereas adding the grille part contributes mostly to the effects seen above 15 kHz. The full black line indicates the effect of removing all complex geometry around the loudspeaker mounting part (especially around the membrane surround and attachment). It is clear that all high-order features are now shifted up in frequency, with the first sharp features occurring well above 15 kHz.

The asymmetric geometry around the mounting part of the loudspeaker, primarily the loudspeaker terminal housing, introduces odd interference patterns which inevitably will affect the resulting sound field radiated into the listening space. A more thorough investigation of the primary effects, causing the radiation features identified in Fig. 6, can be conducted by inspecting sound pressure level distribution inside the interior domain of the simulation. In Fig. 7 this is shown for three frequencies, at where feature B-D occur. The main effects appear to arise due to the geometry of the interface, as already indicated above, and the radiation characteristics are thus subject to change when adapting a different geometrical transition from the loudspeaker membrane to the grille part. It is apparent that optimization of interface geometry can reduce this interaction, and that a cylindrical interface constitutes a convenient (in terms of development) but

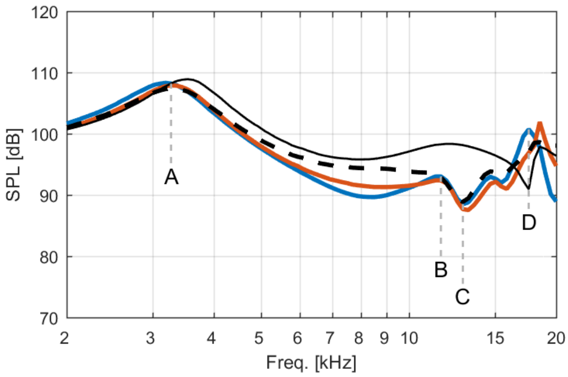


**Fig. 6:** Comparison of on-axis frequency response predictions applying: full 3-D resolved holes (——), 2-D interior perforated plate boundary condition (——), and the case without grille as reference (- - -). A simplified version of the loudspeaker mounting geometry (——) is included for comparison. The points indicated by A-D highlights the main features.

poorly designed wave guide. However, specifically in automotive applications, attention should not only be focused towards minimizing the effect of the interface, but merely towards understanding the acoustic environment adjacent to the loudspeaker. The criterion for achieving a well-integrated solution depends heavily on the position. One can benefit from focusing direct sound away from complex boundary interaction in some cases, whereas other scenarios require less directive sound dispersion. Irrespective of the application,

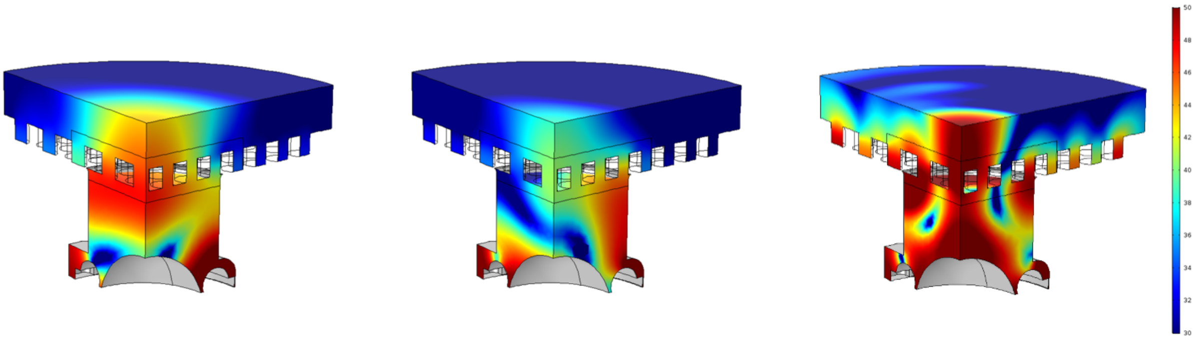

**(a)** $f = 11.6$ kHz. **(b)** $f = 13.2$ kHz. **(c)** $f = 17.5$ kHz.

**Fig. 7:** Sound pressure level plots of one quarter of the interior air-domain comprising the interface between the loudspeaker membrane and the grille part - shown at the frequencies, where the features B-D of the on-axis grille response are found (see Fig. 6).

the acoustic environment inside an automotive interior is heavily influencing the sound field radiated from high frequency loudspeakers, which might reduce the significance of the influence imposed by the grille assembly, relative to the in-situ features in the surrounding area.

## 6 Summary

A validity study was presented, comparing the prediction based on a finite element model and experimental studies, of the acoustical consequences from adding a grille assembly onto a dome tweeter. The results show that numerical modeling can be utilized in rapid assessment of loudspeaker grille assemblies, based on the on-axis frequency response, where the prominent features were identified. The prediction of the resulting directivity was found to agree well with measurements performed in a 2 $\pi$ baffle.

## References

[1] Aretz, M. and Vorländer, M., "Combined wave and ray based room acoustic simulations of audio systems in car passenger compartments, Part I: Boundary and source data," *Applied acoustics*, 76, pp. 82–99, 2014.

[2] Leach Jr, W. M., "Introduction to electroacoustics and audio amplifier design, Kendall," 2003.

[3] Desai, C. S. and Kundu, T., *Introductory finite element method*, CRC Press, 2001.

[4] Ciskowski, R. D. and Brebbia, C. A., *Boundary element methods in acoustics*, Springer, 1991.

[5] Williams, E. G., *Fourier acoustics: sound radiation and nearfield acoustical holography*, Academic press, 1999.

[6] Multiphysics, C., "Acoustics module user's guide version 5.3," *User's manual*, 2017.

[7] Berenger, J.-P., "A perfectly matched layer for the absorption of electromagnetic waves," *Journal of computational physics*, 114(2), pp. 185–200, 1994.

[8] Paul-Schönemann, J., "Power Response Measurement in Non-Reverberant Environments," in *Audio Engineering Society Convention 92*, Audio Engineering Society, 1992.

[9] Farina, A., "Advancements in Impulse Response Measurements by Sine Sweeps," in *Audio Engineering Society Convention 122*, 2007.

[10] Chapman, P. J., "Ambient Atmospheric Conditions and Their Influence on Acoustic Measurements," in *Audio Engineering Society Convention 136*, 2014.